Realization of high-efficiency AlGaN deep ultraviolet light-emitting diodes with polarization-induced doping of the p-AlGaN hole injection layer

Yi-Wei Cao(曹一伟)[1], Quan-Jiang Lv(吕全江)[1,†], Tian-Peng Yang(杨天鹏)[2,3], Ting-Ting Mi(米亭亭)[3], Xiao-Wen Wang(王小文)[3], Wei Liu(刘伟)[3], and Jun-Lin Liu(刘军林)[1,‡]

[1] *School of Materials Science and Engineering, Jiangsu University, Zhenjiang* 212013, *China*
[2] *EpiTop Optoelectronic Co., Ltd, Ma'anshan* 243000, *China*
[3] *Ma'anshan Jason Semiconductor Co., Ltd, Ma'anshan* 243000, *China*

(Received 27 September 2022; revised manuscript received 21 October 2022; accepted manuscript online 27 October 2022)

We investigate the polarization-induced doping in the gradient variation of Al composition in the p-$Al_{0.75}Ga_{0.25}N/Al_xGa_{1-x}N$ hole injection layer (HIL) for deep ultraviolet light-emitting diodes (DUV-LEDs) with an ultra-thin p-GaN (4 nm) ohmic contact layer capable of emitting 277 nm. The experimental results show that the external quantum efficiency (EQE) and wall plug efficiency (WPE) of the structure graded from 0.75 to 0.55 in the HIL reach 5.49% and 5.04%, which are improved significantly by 182% and 209%, respectively, compared with the structure graded from 0.75 to 0.45, exhibiting a tremendous improvement. Both theoretical speculations and simulation results support that the larger the difference between 0.75 and x in the HIL, the higher the hole concentration that should be induced; thus, the DUV-LED has a higher internal quantum efficiency (IQE). Meanwhile, as the value of x decreases, the absorption of the DUV light emitted from the active region by the HIL is enhanced, reducing the light extraction efficiency (LEE). The IQE and LEE together affect the EQE performance of DUV-LEDs. To trade off the contradiction between the enhanced IQE and decreased LEE caused by the decrease in Al composition, the Al composition in the HIL was optimized through theoretical calculations and experiments.

Keywords: deep ultraviolet light-emitting diode (DUV-LED), polarization-induced doping, AlGaN, light extraction efficiency

PACS: 85.60.Jb, 73.61.Ey, 78.20.Bh **DOI:** 10.1088/1674-1056/ac9de7

1. Introduction

As the most promising ultraviolet solid-state light source, AlGaN-based deep-ultraviolet light-emitting diodes (DUV-LEDs) have received extensive attention from researchers.[1–4] Spurred by the COVID-19 pandemic, the demand for DUV-LEDs has been increasing since 2020, owing to their contactless sterilization and disinfection capabilities.[5] Despite the fact that there are enormous open doors for AlGaN-based DUV-LEDs, large-scale commercial applications of AlGaN-based DUV-LEDs still face huge challenges, the most significant being their insufficient external quantum efficiency (EQE) and wall-plug efficiency (WPE).[6–8] Either or both degraded internal quantum efficiency (IQE) and inadequate light extraction efficiency (LEE) are the factors responsible for the insufficient EQE.[9–11]

The reasons for the limited efficiency of AlGaN-based DUV-LEDs are rooted in the fundamental properties of AlGaN material with a high Al content.[12] Achieving a large hole concentration with a high Al content in $Al_xGa_{1-x}N$ alloys is challenging. The Mg activation energy in $Al_xGa_{1-x}N$ alloys increases with increasing Al content, resulting in a lower hole concentration.[13–15] To circumvent the issue of poor hole concentration, efficient approaches include, but are not limited to, using polarization-induced doping and unique band-engineered epistructures to increase hole concentration or manage carrier confinement capabilities.[16,17] For instance, Malik *et al.*[18] introduced a 40 nm thick Al-grade p-AlGaN hole source layer in a 222 nm band far-UVC LED, resulting in an improvement in the radiative recombination rate of up to $\sim$ 124%. Xu *et al.*[19] reported the replacement of a conventional LED structure with a p-AlGaN hole injection layer (HIL) with gradually changing Al composition, resulting in an increase in the near-UV LED optical power of 266%. Moreover, AlGaN-based DUV-LEDs suffer from severe LEE loss compared with InGaN-based LEDs, which is mainly due to the optical polarization of $Al_xGa_{1-x}N$ with high Al content and strong optical absorption of the p-GaN ohmic contact layer.[20–22] Despite the absorption losses being unavoidable on the top surface of the DUV-LEDs, reducing the thickness of the p-GaN contact layer can significantly reduce the absorption losses. For a 50 nm thick p-GaN ohmic contact layer, more than 81% of the DUV light reflected from the metal contact layer can be absorbed (emission peak near 275 nm), but by thinning the p-GaN to 5 nm the absorption losses per reflection

†Corresponding author. E-mail: lvquanjiang@ujs.edu.cn
‡Corresponding author. E-mail: liujunlin@ujs.edu.cn

© 2023 Chinese Physical Society and IOP Publishing Ltd

can be reduced to 16%.[23] It is also worth stating that reducing the thickness of the p-GaN may also result in a lower hole concentration, and adjustments in the epistructure are needed to compensate for this loss.

In this work, with the aims of improving hole injection efficiency of the p-type layer and reducing the absorption of DUV light by p-GaN, AlGaN-based DUV-LEDs with polarization-induced doping of the p-AlGaN HIL and an ultra-thin p-GaN ohmic contact layer were introduced. The proposed structure overcomes the contradiction between the decrease in Mg activation energy and the increase in the DUV light absorption due to the reduction in Al composition in p-AlGaN. Both the experimental and simulation results verify an impressive improvement in the performance of the AlGaN-based LEDs with this proposed structure.

2. Structures and parameters

Figure 1 shows four schematic DUV-LED heterostructures used in this study for comparison. Epistructures were initiated on a 2 inch (0001) AlN template on a sapphire substrate, followed by a 2 μm thick Si-doped n-$Al_{0.48}Ga_{0.52}N$ layer ($n \sim 5.0 \times 10^{18}$ cm^{-3}) as the electron injection layer. After that there is the active region with five pairs of 2.5 nm thick $Al_{0.45}Ga_{0.55}N$ quantum wells and 10 nm thick Si-doped $Al_{0.60}Ga_{0.40}N$ quantum barriers ($n \sim 3.0 \times 10^{18}$ cm^{-3}); the undoped last barrier is 3 nm thick. Then, a 10 nm thick Mg-doped ($p \sim 1.0 \times 10^{18}$ cm^{-3}) p-type $Al_{0.75}Ga_{0.25}N$ electron blocking layer was grown on top of the active region. After that a Mg-doped ($p \sim 3.0 \times 10^{18}$ cm^{-3}) graded p-$Al_{0.75}Ga_{0.25}N/Al_xGa_{1-x}N$ layer (where x is the Al mole fraction) was designed as a polarization-induced doping HIL. Four LED structures have the same thickness of 55 nm for the HIL, while the Al mole fractions corresponding to the end of the HIL were different, i.e., 0.45, 0.50, 0.55, and 0.60 for samples A, B, C, and D, respectively. Next, a 10 nm thick Mg-doped ($p \sim 3.0 \times 10^{19}$ cm^{-3}) p-$Al_xGa_{1-x}N/Al_{0.4}Ga_{0.6}N$ layer followed as a transition layer and the Al mole fraction was linearly decreased from x to 0.40. Finally, an ultra-thin Mg-doped p-GaN layer ($p \sim 2.0 \times 10^{20}$ cm^{-3}) with a thickness of 4 nm was adopted as the ohmic contact layer.

After the epitaxial growth, standard processing steps were performed to fabricate 500 μm × 500 μm flip-chip DUV-LEDs with indium tin oxide and an alloy stack of Ni/Au metals as the p-type electrode for ohmic contact. Subsequently, the chips were partially etched by an inductively coupled plasma dry etching process down to the n-$Al_{0.48}Ga_{0.52}N$ layer, after which a Cr/Al/Ti/Au n-type electrode was evaporated in sequence on the exposed n-$Al_{0.48}Ga_{0.52}N$ layer. The room-temperature light output power and emission spectra of the DUV-LEDs were measured using a calibrated integrating sphere and spectrometer.

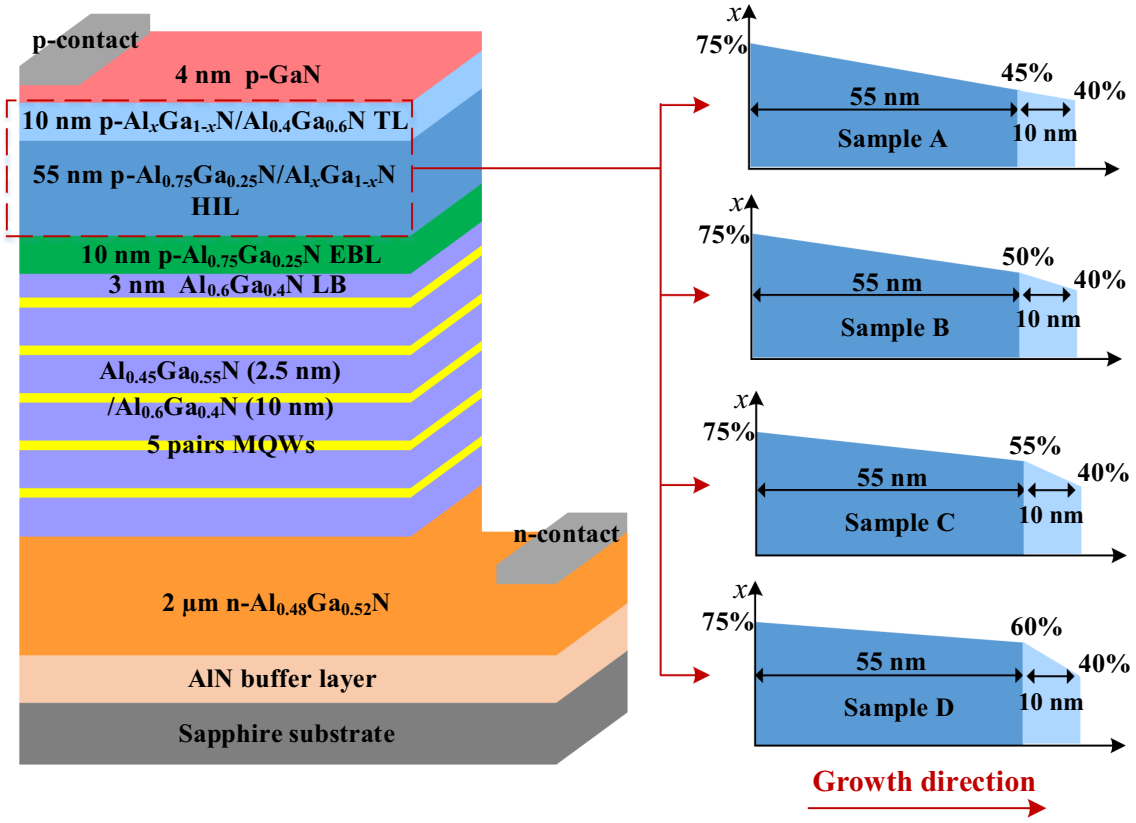


Fig. 1. Schematic structure of an AlGaN-based DUV-LED with different polarization-induced doping HILs (EBL, electron blocking layer; LB, last barrier; MQW, multi-quantum well; TL, transition layer).

In addition, simulations were performed to study the physical mechanisms using the commercial technology computer-aided design (TCAD) simulation program. This program can work on the properties of carrier transport for LED devices by solving the Schrödinger equation, Poisson's equation, drift–diffusion equation and the current continuity equation self-consistently with proper boundary conditions. In consideration of the actual situation in the active region, the Shockley–Read–Hall lifetime and the Auger recombination coefficient are set to be 10 ns and 1.0×10^{-31} $cm^6\cdot s^{-1}$,[24] respectively. The electron and hole mobilities of AlGaN are 250 $cm^2\cdot V^{-1}\cdot s^{-1}$ and 5 $cm^2\cdot V^{-1}\cdot s^{-1}$, while those of GaN are 300 $cm^2\cdot V^{-1}\cdot s^{-1}$ and 10 $cm^2\cdot V^{-1}\cdot s^{-1}$.[25] The energy band offset ratio $\Delta E_c/\Delta E_v$ is 0.7/0.3 for III-nitride material systems.[26] Other parameters for group III-nitride semiconductors can be found in the literature.[27]

3. Results and discussion

Figure 2(a) presents the secondary ion mass spectroscopy depth profiles of Al, Ga, and Mg concentrations in the upper part of sample C ($x = 0.55$). From the distribution profiles of the Ga and Al atoms in the graded p-$Al_{0.75}Ga_{0.25}N/Al_{0.55}Ga_{0.45}N$ HIL it can be clearly seen that along the growth direction the Al atom distribution shows a gradually decreasing trend while the Ga atom distribution shows a gradually increasing trend; this is strong proof that this gradient structure is exactly what we designed. Furthermore, from the Mg distribution profile we can observe that the Mg acceptor concentration in the p-type layer has two distinct levels. The upper GaN is doped with more Mg atoms in order to achieve good ohmic contact. Prior to the p-GaN section, we can observe that the doping of the Mg acceptor increases with decreasing Al composition in the polarization-induced doped p-$Al_{0.75}Ga_{0.25}N/Al_{0.55}Ga_{0.45}N$ layer. At the interface between GaN:Mg and AlGaN:Mg, the Mg-related signal points to a higher Mg concentration of 2.0×10^{20} cm^{-3}. For the p-$Al_{0.75}Ga_{0.25}N/Al_{0.55}Ga_{0.45}N$ layer, a Mg concentration of $(2–3)\times10^{18}$ cm^{-3} is confirmed, which is consistent with the designed value. Figure 2(b) shows an atomic force microscope (AFM) image of the surface of sample C. This confirms that the ultrathin 4 nm p-GaN ohmic contact layer possesses a flat surface. The root mean square value of the surface roughness of the surface (p-GaN) obtained from the AFM image was 3.83 nm.

Figures 3(a) and 3(b) show the experimental results for the forward current-dependent light output power (LOP) and EQE characteristics of the four DUV-LED structures, respectively. Obviously, graded p-$Al_{0.75}Ga_{0.25}N/Al_xGa_{1-x}N$ layers with different Al molar fractions have a significant impact on both the LOP and EQE performances. As depicted in Fig. 3(a), the LOP does not increase linearly with increase in the Al molar fraction in the p-$Al_{0.75}Ga_{0.25}N/Al_xGa_{1-x}N$ HIL, but shows an explicit trend of increasing and then decreasing. Specifically, at an injection current of 300 mA, the LOPs of samples A, B, C, and D are 28.2 mW, 30.4 mW, 45.8 mW, and 31.7 mW, respectively. The inset of Fig. 3(a) shows the room-temperature electroluminescence spectra of the four DUV-LED structures at 100 mA. The peak wavelength of all samples is around 277 nm, and sample C has the highest emission intensity, almost twice as high as that of sample A. In Fig. 3(b), the EQE curves of the four DUV-LED structures show a typical efficiency droop behavior, but they exhibit different droop ratios. The EQE peaks of the four structures are 3.01%, 3.71%, 5.49%, and 4.17%, occurring at an injection current of 10 mA, respectively. The inset of Fig. 3(b) shows the maximum WPE values of the four structures, which are 2.41%, 3.11%, 5.04%, and 3.70%, respectively. The maximum EQE and WPE of sample C increased by 182% and 209% compared with sample A, exhibiting a significant improvement. In Fig. 3(c), the DUV-LEDs with the ultra-thin 4 nm p-GaN have an average voltage of about 5.6 V–6.1 V at 40 mA, which is similar to the commercial inverted DUV-LEDs reported in Ref. [28]. Obviously, sample C with an Al compositional grading from 0.75 to 0.55 in the p-$Al_{0.75}Ga_{0.25}N/Al_xGa_{1-x}N$ HIL exhibits a remarkable performance enhancement.

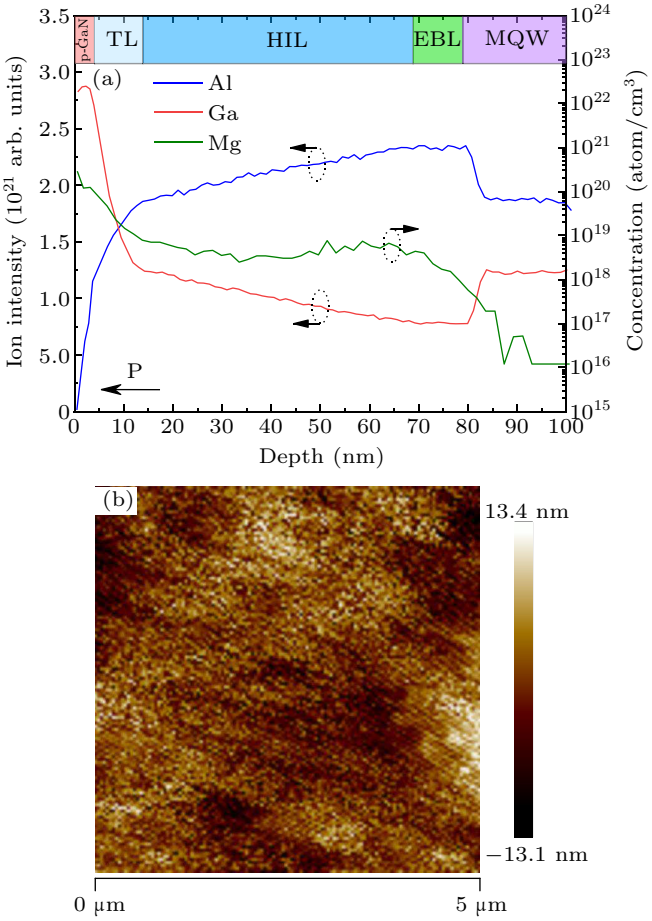


Fig. 2. (a) Depth profiles of Al, Ga, and Mg probed by secondary ion mass spectroscopy from the upper part of sample C and (b) the 5 μm × 5 μm atomic force microscopy image of the surface (p-GaN) of sample C.

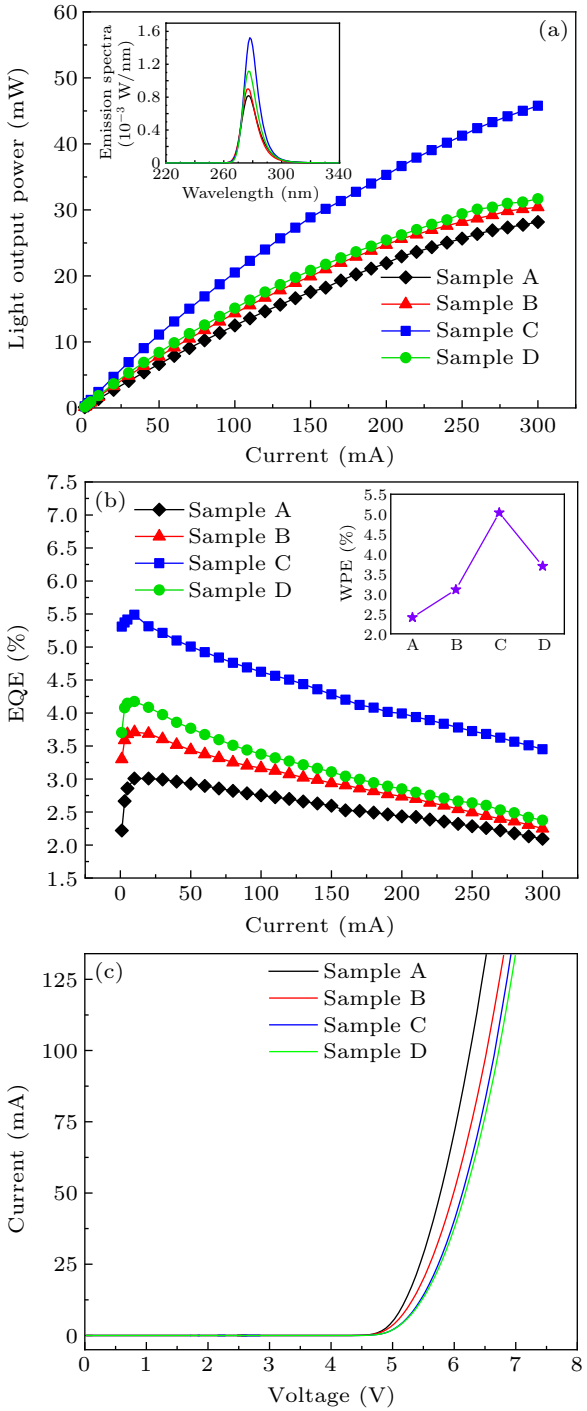


Fig. 3. The experimental results of (a) light output power and (b) EQE as a function of injection current. (c) *I*–*V* curves for samples A, B, C, and D. The insets in (a) and (b) show the electroluminescence emission spectra (at 100 mA) and the maximum WPE of the four samples, respectively.

To better understand the physical mechanisms that affect device performance when varying the Al composition in the graded p-$Al_{0.75}Ga_{0.25}N/Al_xGa_{1-x}N$ HIL, we take the schematic model shown in Fig. 4. Hole formation in the Al composition graded p-AlGaN region due to polarization has been well recognized.[17] As depicted in Fig. 4, the upper AlGaN layer suffers from compressive strain due to lattice mismatch with the high Al composition. Therefore, negative sheet charges are generated at its upper surface, while equivalent positive sheet charges are generated at the lower surface due to piezoelectric and spontaneous polarization. However, the sheet charge strength generated by polarization decreases linearly with decreasing Al composition in the p-$Al_{0.75}Ga_{0.25}N/Al_xGa_{1-x}N$ HIL. However, due to the graded decrease of Al composition from p-$Al_{0.75}Ga_{0.25}N$ to p-$Al_xGa_{1-x}N$ ($x < 0.75$), a net resultant negative unbalanced bound polarization charge is generated over the graded p-$Al_{0.75}Ga_{0.25}N/Al_xGa_{1-x}N$ region. To neutralize the negative unbalanced bound polarization charges, holes are consequently generated by acceptor-like impurities or defects through field-assisted ionization, ultimately achieving high-density hole concentration in the HIL. From the above analysis, it is clear that the larger the difference between 75% and x the higher the concentration of negatively polarized charges, and the higher the concentration of holes in the corresponding HIL should be. In addition, the nature of polarization-induced doping leads to a movable three-dimensional hole gas (3DHG) in the continuously graded AlGaN layer.[29] The smaller value of x in the p-$Al_{0.75}Ga_{0.25}N/Al_xGa_{1-x}N$ HIL increases the concentration of the 3DHG, which improves the migration of holes to the active region and achieves a higher hole injection efficiency for the p-type layer. However, contrary to the above analysis, the results in Fig. 3 show an unanticipated phenomenon. Namely, sample A has the smallest x, the hole concentration in the HIL should be the largest and the LOP should be better, but in fact sample A has the worst LOP performance.

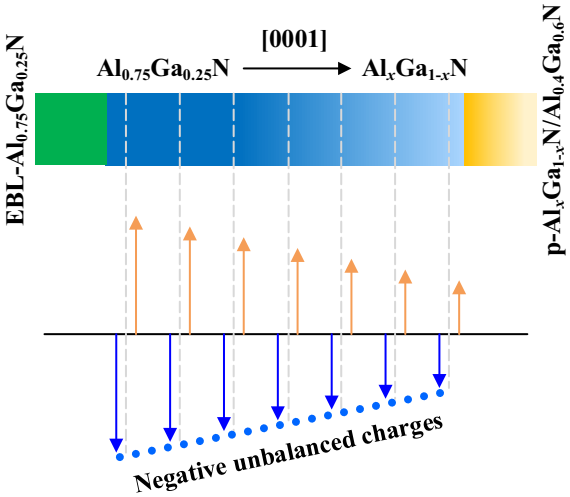


Fig. 4. Schematic model of the polarization sheet charge generation at interfaces of the graded Al composition HIL. Positive and negative charges are indicated by the upward arrows in yellow and downward arrows in blue, respectively.

To gain more insight into the effect of polarization-induced doping of the p-AlGaN HIL on the LOP of four samples, the simulation results in Fig. 5 are presented for further demonstration. Figure 5(a) presents the IQE characters of the four devices as a function of current density (up to

$J = 200$ A·cm^{-2}). As depicted in Fig. 5(a), in the low current density region, the IQE values of the four samples rapidly rise to the maximum value, and that of sample A is the largest. In addition, the results in Fig. 5(a) also clearly show that the IQE of the four samples decreases sequentially with the increase of the x value in the p-Al$_{0.75}$Ga$_{0.25}$N/Al$_x$Ga$_{1-x}$N HIL over the entire current density range, which is consistent with the previous analysis.

Figures 5(b)–5(d) further show the radiative recombination rate, electron concentration and hole concentration within the active region of four structures at a current density of 75 A·cm^{-2}, respectively. For better observation, except for sample A, the x-axis coordinates of the curves of the other three samples are intentionally increased by a certain value. As depicted in Fig. 5(c), the electron distribution among the quantum wells (QWs) of the four structures is similar, especially in the two QWs near the n-side. This can be interpreted as showing that the polarization-induced doping of the p-type HIL has a weak effect on the electron distribution in the active region. Figure 5(d) shows the hole concentration distribution profiles in the QWs of four structures; it reveals that most of the holes are accumulated in the QWs next to the p-type region due to the high effective mass and low mobility, which is similar to the results obtained for InGaN-based LEDs.[30] The result for hole concentration distribution in Fig. 5(d) shows that the hole concentrations of samples A, B, C, and D decrease sequentially, and this difference becomes more pronounced in the QWs close to the p-type region. This result is consistent with our previous inference that in the polarization-induced doping of the p-Al$_{0.75}$Ga$_{0.25}$N/Al$_x$Ga$_{1-x}$N HIL, the smaller the value of x, the higher the hole concentration in the QWs. Figure 5(b) shows the corresponding radiative recombination rate of the four structures. Generally, spontaneous emission is limited by the hole concentration, since they are the minority carriers in the active region. As indicated in Fig. 5(d), for samples with a smaller x value the hole concentration in the QWs is significantly enhanced, which in turn leads to an increase in the radiative recombination rate. Under this circumstance, it is not surprising that the radiative recombination rate of samples A, B, C, and D decreases sequentially.

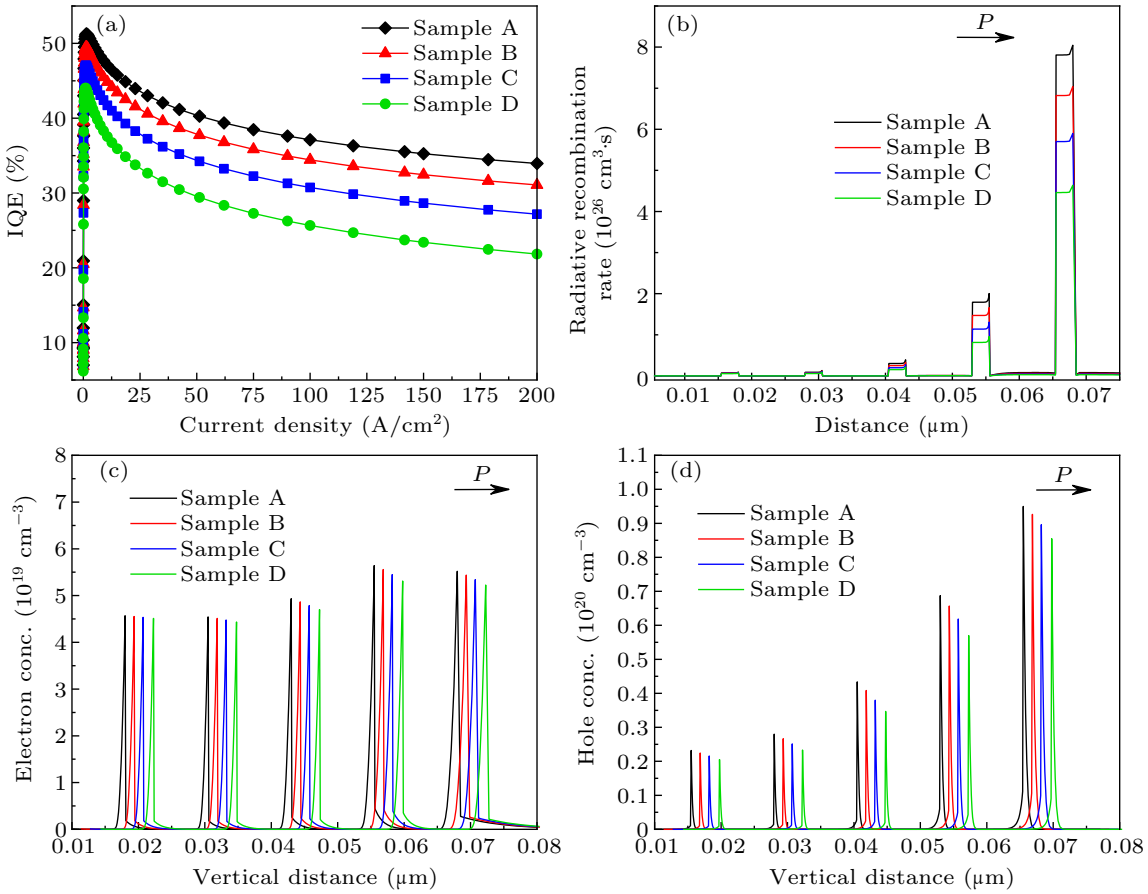


Fig. 5. The calculated results for (a) IQE as a function of current density for four samples, (b) radiative recombination rate, (c) electron concentration and (d) hole concentration profiles within the active region at a current density of 75 A·cm^{-2} for samples A, B, C, and D.

Although both the theoretical speculations and simulation results in Fig. 5 support that samples with smaller x should have a higher radiative recombination rate this is not consistent with the experimental results presented by the EQE curves in Fig. 3(b). The results in Fig. 3(b) show that for samples A, B, C, and D, the EQE first increases and then decreases with increasing x value, implying that there are other factors that affect the EQE performance. As is well known, EQE is the

product of IQE and LEE, where LEE refers to the light extraction efficiency. Unlike InGaN-based blue LEDs, AlGaN-based DUV-LEDs have a strong self-absorption effect. Most of the light emitted from the active region is confined and reabsorbed inside the device, severely reducing the LEE. Obviously, the simulated IQE results do not take this into account. The absorption of DUV light at specific wavelengths by AlGaN bulk materials depends mainly on the thickness and Al molar fraction.[31,32] The intrinsic absorption that occurs in semiconductor materials requires that the photon energy must be equal to or greater than the energy band-gap (E_g). The relationship between the intrinsic absorption wavelength λ_0 and E_g can be derived as λ_0 (nm) $= 1240/E_g$ (eV). In addition, it is known from Vegard's law that E_g of $Al_xGa_{1-x}N$ materials at room temperature can be regulated by modulating the Al molar fraction (x), and the relationship between them can be expressed as

$$E_g\,(Al_xGa_{1-x}N) = xE_g\,(AlN) + (1-x)E_g\,(GaN) - bx(1-x), \tag{1}$$

where E_g(AlN) and E_g(GaN) denote the room temperature energy band gaps of AlN and GaN, taken as 6.28 eV and 3.42 eV, respectively,[33] and b is the band gap bowing parameter, which has been reported to take values from −0.8 eV to 2.6 eV due to the strain present in AlGaN. Here, on the basis of previous reports and the real growth conditions of the designed AlGaN-based DUV-LED, the AlGaN band bowing parameter is taken as 0.7 eV.[34,35] According to Eq. (1), it can be calculated that DUV light at 277 nm is absorbed when the Al composition in p-$Al_xGa_{1-x}N$ is about 0.45, which is equal to the Al composition of the AlGaN QWs in the active region, as shown in Fig. 6.

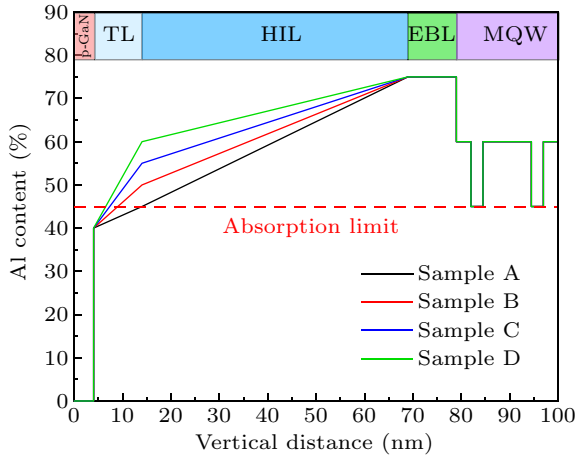


Fig. 6. Schematic diagram of the absorption limit as a function of the Al content in the p-type layer of samples A, B, C, and D.

It can be seen from Fig. 6 that the part below the absorption limit has strong absorption for DUV light near 277 nm, and the farther away from the absorption limit, the stronger the absorption. As depicted in Fig. 1, the p-type layer, which includes the HIL, transition layer and ohmic contact layer, is usually made of Mg-doped p-AlGaN and p-GaN with a band gap smaller than the QW band gap, and hence absorption occurs. Therefore, sample A has the greatest absorption thickness, and absorbs more strongly at the absorption site, and has the lowest LEE. Sample D has the smallest absorption thickness and the highest Al composition in the AlGaN segment of the absorption, i.e., the weakest absorption of DUV light at 277 nm, and has the highest LEE. Accordingly, it is reasonable to speculate that the reabsorption of DUV light by the p-type layer leads to a decrease in LEE and forms a key link behind-the-scenes in the decrease in EQE when the sample has a high IQE.

4. Conclusion

In conclusion, AlGaN-based DUV-LEDs with a p-$Al_{0.75}Ga_{0.25}N$/$Al_xGa_{1-x}N$ polarization-induced doping HIL have been investigated experimentally and numerically. When the Al composition in the polarization-induced doping HIL was gradually decreased from 0.75 to 0.55 (sample C) we achieved maximum EQE and WPE of 5.49% and 5.04%, respectively; these are enhanced significantly by 182% and 209%, respectively, compared with sample A ($x = 0.45$). It has been demonstrated that the larger the difference between 0.75 and x in the HIL, the higher the hole concentration that should be induced. Thus, the DUV-LED has a higher IQE. Therefore, the simulation results show that sample A has the maximum IQE. However, the lower the Al composition in the HIL, the more severe the absorption of the p-type layer, which reduces the LEE. Therefore, even though samples A and B have a higher IQE, their EQE and WPE performances are still poor. In addition, the polarization-induced doping structures with an ultra-thin 4 nm p-GaN ohmic contact layer reduce the absorption of DUV light by the p-type layer without affecting the hole injection efficiency, and the average voltage of the devices is about 5.6 V–6.1 V at 40 mA.

Acknowledgments

Project supported by the National Natural Science Foundation of China (Grant No. 62104085) and the Innovation/Entrepreneurship Program of Jiangsu Province, China (Grant No. JSSCTD202146).

References

[1] Kneissl M, Seong T Y, Han J and Amano H 2019 *Nat. Photon.* **13** 233
[2] Wang T Y, Lai W C, Sie S Y, Chang S P, Wu Y R, Chiou Y Z, Kuo C H and Sheu J K 2020 *Appl. Phys. Lett.* **117** 251101
[3] Sun Y H, Xu F J, Xie N, Wang J M, Zhang N, Lang J, Liu B Y, Fang X Z, Wang L B, Ge W K, Kang X N, Qin Z X, Yang X L, Wang X Q and Shen B 2020 *Appl. Phys. Lett.* **116** 212102
[4] Li Y, Ge M, Wang M, Zhu Y and Guo X 2022 *Chin. Phys. B* **31** 077801

[5] Raeiszadeh M and Adeli B 2020 *ACS Photonics* **7** 2941

[6] Park J S, Kim J K, Cho J and Seong T Y 2017 *ECS J. Solid State Sci. Technol.* **6** Q42

[7] Lobo-Ploch N, Mehnke F, Sulmoni L, Cho H K, Guttmann M, Glaab J, Hilbrich K, Wernicke T, Einfeldt S and Kneissl M 2020 *Appl. Phys. Lett.* **117** 111102

[8] Zhang C, Hui-Qing S, Li X N, Sun H, Fan X C, Zhang Z D and Guo Z Y 2016 *Chin. Phys. B* **25** 028501

[9] Djavid M and Mi Z 2016 *Appl. Phys. Lett.* **108** 051102

[10] Lang J, Xu F J, Ge W K, Liu B Y, Zhang N, Sun Y H, Wang M X, Xie N, Fang X Z, Kang X N, Qin Z X, Yang X L, Wang X Q and Shen B 2019 *Appl. Phys. Lett.* **114** 172105

[11] Liu D, Cho S J, Park J, Gong J, Seo J H, Dalmau R, Zhao D, Kim K, Kim M, Kalapala A R K, Albrecht J D, Zhou W, Moody B and Ma Z 2018 *Appl. Phys. Lett.* **113** 011111

[12] Bharadwaj S, Islam S M, Nomoto K, Protasenko V, Chaney A, Xing H and Jena D 2019 *Appl. Phys. Lett.* **114** 113501

[13] Jiang K, Sun X, Shi Z, Zang H, Ben J, Deng H X and Li D 2021 *Light Sci Appl* **10** 69

[14] Chen Y, Wu H, Han E, Yue G, Chen Z, Wu Z, Wang G and Jiang H 2015 *Appl. Phys. Lett.* **106** 162102

[15] Li G, Wang L Y, Song W D, Jiang J, Luo X J, Guo J Q, He L F, Zhang K, Wu Q B and Li S T 2019 *Chin. Phys. B* **28** 058502

[16] Liang Y H and Towe E 2018 *Appl. Phys. Rev.* **5** 011107

[17] Simon J, Protasenko V, Lian C, Xing H and Jena D 2010 *Science* **327** 60

[18] Malik S, Usman M, Khan M A and Hirayama H 2021 *J. Mater. Chem. C* **9** 16545

[19] Xu M, Zhou Q, Zhang H, Wang H and Zhang X 2016 *Superlattices Microstruct.* **94** 25

[20] Zhang D, Chu C, Tian K, Kou J, Bi W, Zhang Y and Zhang Z H 2020 *AIP Adv.* **10** 065032

[21] Ni R, Yu Z, Liu Z, Zhang L, Jia L and Zhang Y 2020 *IEEE Photonics Technol. Lett.* **32** 971

[22] Huang C Y, Tsai C L, Huang C Y, Yang R Y, Wu Y S, Yen H W and Fu Y K 2020 *Appl. Phys. Lett.* **117** 261102

[23] Kneissl M 2016 *III-Nitride Ultraviolet Emitters* (Switzerland: Springer)

[24] Chee K W A, Guo W, Wang J R, Wang Y, Chen Y E and Ye J 2018 *Mater. Des.* **160** 661

[25] Sakowski K, Marcinkowski L, Krukowski S, Grzanka S and Litwin-Staszewska E 2012 *J. Appl. Phys.* **111** 123115

[26] Pandey A, Shin W J, Liu X and Mi Z 2019 *Opt. Express* **27** A738

[27] Manikandan M, Nirmal D, Ajayan J, Arivazhagan L, Prajoon P and Dhivyasri G 2020 *Opt. Quantum Electron.* **52** 513

[28] Trivellin N, Monti D, Piva F, Buffolo M, De Santi C, Zanoni E, Meneghesso G and Meneghini M 2019 *Jpn. J. Appl. Phys.* **58** SCCC19

[29] Zhang L, Ding K, Yan J C, Wang J X, Zeng Y P, Wei T B, Li Y Y, Sun B J, Duan R F and Li J M 2010 *Appl. Phys. Lett.* **97** 062103

[30] Jin-Wei S, Shi-Hao G, Lin C S, Jinn-Kong S, Kuo-Hua C, Lai W C, Kuo C H, Tun C J and Jen-Inn C 2009 *IEEE J. Sel. Top. Quantum Electron.* **15** 1292

[31] Yu H, Ren Z, Zhang H, Dai J, Chen C, Long S and Sun H 2019 *Opt. Express* **27** A1544

[32] Jo M, Maeda N and Hirayama H 2016 *Appl. Phys. Express* **9** 012102

[33] Pelá R R, Caetano C, Marques M, Ferreira L G, Furthmüller J and Teles L K 2011 *Appl. Phys. Lett.* **98** 151907

[34] Nepal N, Li J, Nakarmi M L, Lin J Y and Jiang H X 2005 *Appl. Phys. Lett.* **87** 242104

[35] Beladjal K, Kadri A, Zitouni K and Mimouni K 2021 *Superlattices Microstruct.* **155** 106901